Monte Carlo study of picosecond exciton relaxation and dissociation in poly(phenylenevinylene)

M. Scheidler* and U. Lemmer†
Fachbereich Physik, Fachbereich Physikalische Chemie, and Zentrum für Materialwissenschaften der Philipps-Universität Marburg, Renthof 5, D-35032 Marburg, Germany

R. Kersting‡
Institut für Halbleitertechnik II, Rheinisch-Westfalische Technische Hochschule Aachen, Sommerfeldstrasse 24, 52074 Aachen, Germany

S. Karg§ and W. Riess‖
Physikalisches Institut, LP II and BIMF, Universität Bayreuth, 95440 Bayreuth, Germany

B. Cleve and R. F. Mahrt
Fachbereich Physik, Fachbereich Physikalische Chemie, and Zentrum für Materialwissenschaften der Philipps-Universität Marburg, Renthof 5, D-35032 Marburg, Germany

H. Kurz
Institut für Halbleitertechnik II, Rheinisch-Westfalische Technische Hochschule Aachen, Sommerfeldstrasse 24, 52074 Aachen, Germany

H. Bässler, E. O. Göbel,¶ and P. Thomas
Fachbereich Physik, Fachbereich Physikalische Chemie, and Zentrum für Materialwissenschaften der Philipps-Universität Marburg, Renthof 5, D-35032 Marburg, Germany

(Received 4 March 1996)

We present a Monte Carlo study of the relaxation and dissociation dynamics of optical excitations in poly(p-phenylenevinylene). The quantitative comparison with experimental data gives a complete picture of the excitation dynamics, the relevant parameters of the spectral relaxation, and the trapping processes involved. Our simulations are extended to include the primary step of the dissociation of a neutral photoexcitation in an electric field. The comparison with the results of field-induced photoluminescence quenching experiments enables us to understand the dissociation dynamics and to determine the exciton binding energy to 0.3 ± 0.1 eV. [S0163-1829(96)05128-4]

I. INTRODUCTION

The photophysics of conjugated polymers is currently extensively investigated due to the interesting physical properties of these materials[1] as well as their large potential for electroluminescence applications.[2] Among the class of fluorescent conjugated polymers poly(p-phenylenevinylene) (PPV) has attracted much attention since the initial demonstration of electroluminescence (EL) in a diode based on this material.[3] Several experimental investigations have recently contributed to a deeper understanding of the nature and the dynamics of the excited electronic states of this π-conjugated polymer.[4–7] It was shown that the disorder present in the polymers leads to a localization of the electronic wave function and the formation of a fairly broad density of states (DOS).[8] The ultrafast dynamics of the photoexcitations in PPV has been qualitatively explained by a spectral relaxation within this DOS.[9] The details and the relevant parameters of the incoherent hopping motion, however, are still unknown. It has been pointed out that the decay of the photoexcitations is strongly affected by trapping of mobile excitations at nonradiative centers leading to excitation annihilation and thus to a reduction of the quantum efficiency in photoluminescence (PL) and EL experiments.[10,11] It is evident that the performance of conjugated polymers in optoelectronic devices as light-emitting diodes, photodetectors, and solar cells is determined by the transport dynamics of excitations and the generation of charge carriers. A quantitative understanding of the relaxation and dissociation processes is therefore of fundamental importance for the design and improvement of polymer devices.

The relaxation of neutral excitations in an inhomogeneously broadened DOS has been treated theoretically via several methods.[12,13] On the other hand, a variety of literature exists on the related problem of the trapping dynamics in donor-acceptor systems.[14–16] A superposition of both processes occurs in PPV, thus a unified treatment has to be applied to model the excitation dynamics in this material. Monte Carlo (MC) simulations are well suited for such a problem, since they are easily applicable to a wide variety of model systems.

A key issue in the field of conjugated polymers is the role of electron-electron interactions.[17] It is heavily debated how Coulomb and correlation effects modify the one-electron model based on the Su-Schrieffer-Heeger Hamiltonian.[18] Optical experiments under the influence of an electric field have significantly contributed to this issue in the case of polydiacetylene.[19,20] It was found that the lowest absorption band has to be attributed to an excitonic transition, whereas the band-to-band transition is located at about 0.4 eV higher

in energy. In PPV, the transition from a neutral photoexcitation to a charge carrier has been studied in photocurrent experiments. However, similar experimental findings were explained with rather contradictory values for the exciton binding energy ranging from less than 25 meV (Ref. 21) up to 1.1 eV.[22]

Recently, the dissociation of a neutral excitation in an electric field was investigated by the method of PL quenching. By performing this experiment in a time-resolved manner, the dynamics of the primary step during the transition from a neutral excitation to a pair of charge carriers has been monitored directly.[23,24] Since these experiments have supplied direct data on the dissociation process, a theoretical analysis of these experiments should yield significant information about the size of the exciton binding energy and the microscopic processes involved.

In this paper we use MC simulations for modeling the relaxation, trapping and dissociation dynamics of optical excitations in the conjugated polymer PPV. By comparing the simulation results with time-resolved luminescence experiments we find that the trap density is as high as 20%. Furthermore, we show that the capture into traps is determined by a hopping rate that depends exponentially on the distance between the excitation and the trapping site. These findings indicate that the fluorescence annihilation is due to a phonon-assisted tunneling process of one charge carrier to the trapping site, thereby dissociating the neutral excitation. The role of spatial disorder and dimensionality during the femtosecond relaxation processes is discussed. We complete our work with the simulation of the field-induced dissociation of a neutral photoexcitation. MC calculations of competing energy relaxation, trapping, and exciton dissociation in an external electric field explain our experimental results quantitatively. The computed data show that the exciton binding energy in PPV is 0.3 ± 0.1 eV.

The paper is organized as follows. In Sec. II we describe our model and the details of the MC simulations. A comparison of the simulation and the experimental data addressing the energy relaxation and the trapping processes is presented in Sec. III. In Sec. IV the field-induced dissociation process is discussed in detail. The paper is concluded in Sec. V.

II. MODEL AND SIMULATIONS

There is considerable evidence that conjugated polymers can be regarded as arrays of chromophores that can be identified as fully conjugated segments of the polymer chain consisting of 6–10 monomer units in the case of PPV.[8,25] The inset of Fig. 1 shows the chemical structure of the fundamental repeat unit. The electronic and optical properties of the conjugated polymer are determined by the ensemble of conjugated segments, whose optical transitions are similar to those of oligomeric model compounds with comparable length.

In our simulation each site of a 64^3 cubic lattice with a lattice constant a represents a fully conjugated segment. Periodic boundary conditions are employed to prevent finite-size effects. In order to simulate the spatial disorder present in the samples each site is shifted by a random vector $\mathbf{v}$. The value $u = v_{\max}/a$ indicates the degree of spatial disorder and is referred to as ''disorder parameter'' in the following. The

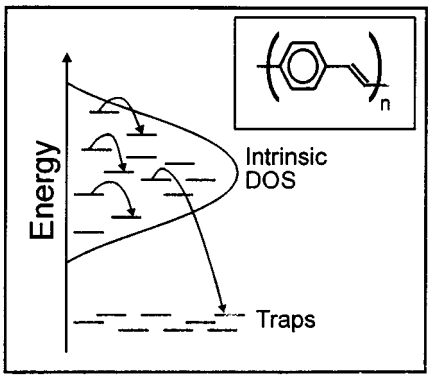

FIG. 1. Energy scheme of our model. We consider hopping processes within the intrinsic density of states as well as trapping processes. The trapping states are located significantly below the intrinsic states. The inset shows the fundamental monomer unit of the polymer.

energetic disorder responsible for the inhomogeneous broadening of the $S_1 - S_0$ (0-0) transition is simulated by assigning random energies to the sites according to a Gaussian distribution. The dotted line in Fig. 2 illustrates the DOS we have used in our simulations in comparison with the absorption and the emission (PL) spectrum. A Gaussian width of $\sigma = 0.08$ eV and a center energy of 2.565 eV for the disorder-broadened DOS is obtained from a fit to the lowest band of the absorption spectrum, which is attributed to the purely electronic transition. At higher photon energies the absorption is due to vibronic side bands. It has been shown previously that the vibronic relaxation after photoexcitation into the vibronic bands takes place on an ultrafast time scale (<300 fs).[9] Since this is faster than the time resolution of the experiments discussed here, we only have to consider electronic relaxation processes. The emission spectrum shown in Fig. 2 exhibits vibronic sidebands on the low-energy side of

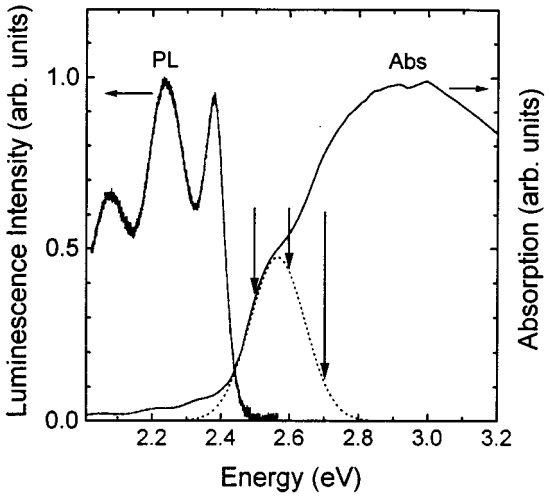

FIG. 2. Time-integrated absorption (Abs) and luminescence spectrum (PL) of the PPV sample. The vertical arrows indicate the different detection energies in the time-resolved luminescence measurements. The density of states (dotted line) for the 0-0 transition is also shown for comparison.

the purely electronic transition. The energetic width of the bands, however, is significantly smaller than in the absorption spectrum. This is due to the relaxation processes that populate the low-energy states of the DOS prior to radiative deactivation into the electronic ground state. The dynamics of these spectral relaxation processes is discussed in detail in this paper.

Further complications arise from the presence of nonradiative trapping processes that compete with the radiative recombination.[10] We simulate traps by introducing sites energetically well below the intrinsic DOS. The energetic scheme of our model is summarized in Fig. 1.

A simulation run of the relaxation dynamics starts with the generation of an ensemble of up to 40 000 excitations randomly distributed over all sites at a time t_0. For the simulation one has to consider different processes as possible candidates for the incoherent excitation transfer because hopping in a disordered solid can be mediated via different microscopic mechanisms. Energy transfer due to a dipole-dipole interaction is one possibility. On the other hand phonon-assisted tunneling of either the neutral excitation or one single charge also has to be taken into account. In general, the hopping rates have the form

$$\nu_{ij}=\nu_0 f(r_{ij})\begin{cases}1, & E_i-E_j>0\\ \exp\left(\dfrac{-\Delta E_{ij}}{kT}\right), & E_i-E_j\leqslant 0\end{cases} \tag{1}$$

with the attempt to escape frequency ν_0. E_i and E_j are the energies of the sites i and j, respectively. ΔE_{ij} is their difference and r_{ij} is the distance between the sites involved. The term $f(r_{ij})$ depends only on the distance between the donating and accepting site. For the phonon-assisted tunneling process the rate for a hop from site i to site j is assumed to be of the Miller-Abrahams type[26] with

$$f_{\mathrm{PAT}}(r_{ij})=\exp\left(\frac{-2r_{ij}}{\alpha}\right), \tag{2}$$

where α is the localization length. In our simulations we use $\alpha=0.2a$, corresponding to 6 Å for a lattice constant of 30 Å .

The same temperature dependence is used for the rates describing the dipole-dipole coupling. For this process the distance dependence is calculated according to[27]

$$f_{\mathrm{dip}}(r_{ij})=\left(\frac{a}{r_{ij}}\right)^6. \tag{3}$$

For an excitation at site i the transfer rates to any site j within a radius $r_{ij}<6a$ is calculated. Other sites can be neglected, since the transfer rates to these sites are, in general, much lower than the inverse radiative lifetime of the excitations. The total rate for the deactivation of site i is then

$$N_i=\sum_j \nu_{ij}+\nu_{i,\mathrm{rec}}, \tag{4}$$

where $\nu_{i,\mathrm{rec}}$ is the radiative recombination rate, assumed to be 10^9 s^{-1}.[10] A dwelling time is attributed to an excitation on site i by

$$t_i=-N_i^{-1}\ln w_i, \tag{5}$$

with a random number $w_i\epsilon[0;1]$, corresponding to an exponential decay with lifetime $\tau_i=N_i^{-1}$.[28]

In agreement with previous work we have neglected bimolecular interactions of the excitations, since the excitation densities in our experiments are lower than 10^{19} cm^{-3}. This simplification reduces the CPU time needed for the simulation drastically. After calculating the dwelling time for all excitations the actual process is chosen according to the corresponding probabilities. This process is carried out and the system is updated. Then the procedure starts again. In more mathematical terms our MC simulation solves numerically the rate equation of the system, as can be shown in close analogy to Ref. 29.

III. EXCITON RELAXATION IN PPV

We start our comparison of computational and experimental results with a discussion of femtosecond relaxation phenomena observed in luminescence upconversion experiments.[9] In these measurements the transient luminescence is detected at different spectral positions around the center of the S_1-S_0 (0.0) transition of PPV located at 2.565 eV. The arrows in Fig. 2 indicate the locations of the different energies where the luminescence was detected. The spectrally dependent transient luminescence intensity measured in the experiments reflects the transient density of neutral excitations at the different energetic positions. Therefore we have computed the transient excitation density of all sites within a certain energy range equal to the experimental spectral resolution ($\approx$30 meV) and now compare the result with the measured decay functions. As a reference curve we always use the experimental luminescence transient at 2.7 eV. Since the depopulation of these states at the high-energy end of the DOS is mainly due to next neighbor downward hops, it does not critically depend on the microscopic hopping mechanism and the density of traps. The first step in a fitting procedure is therefore to find nearest neighbor hopping rates that yield a calculated curve that fits the high-energy luminescence decay. A typical calculated decay pattern is shown in Fig. 3. The transient excitation density at the three different energies as a result of a simulation run without any spatial disorder and any traps assuming a dipole-dipole interaction is depicted. Only hopping and the radiative decay of an excitation with a rate of 10^9 s^{-1} are considered. At an energy of 2.7 eV (at the high-energy end of the DOS) nearly all excitations have six nearest-neighbor sites with lower energies. All of these sites with equal distance can act as an acceptor, leading to a fast exponential decay. At 2.6 eV the decay is slower, since some of the neighboring sites are higher in energy and thus only activated hops to these sites are allowed. At energies below the center of the DOS (2.5 eV) the transient excitation density is dominated by ''filling-up processes'' due to excitations hopping downward from higher energies.

A. Traps

Previous investigations have indicated that trapping plays an important role for the excitation dynamics in PPV.[10] For fitting the experimental data, trap states have to be included

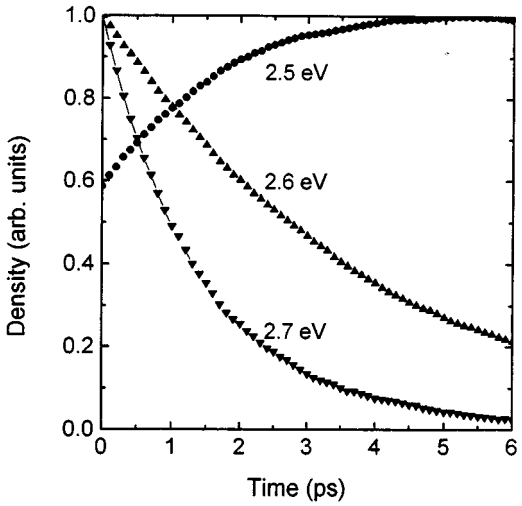

FIG. 3. Calculated transient density of excitations at different energies in the absence of spatial disorder and traps. For the hopping process dipole-dipole coupling with $\nu_0 = 3.3 \times 10^{11}\ s^{-1}$ and a lattice constant of $a = 30$ Å was assumed.

in the simulations. By a quantitative comparison with the experimental data the density of traps can be determined. The inclusion of traps is particularly important for the temporal behavior of the emission at lower energies within the DOS. As shown by the lines in Fig. 4; the temporal maximum of the calculated low-energy luminescence transient at 2.5 eV moves towards shorter times with increasing concentration of traps. This is due the competition between the capture into traps and the spectral relaxation towards intrinsic low-energy sites. From the absence of a distinct delayed maximum in the experimental luminescence transient at 2.5 eV we have to conclude that a rather high density of traps is present in the samples. As shown in Fig. 4, we achieve good agreement of experimental and computational data with the assumption of a trap density of 20% of all sites. It is important to note that this finding does not depend on the assumption for the nature of the transfer process.

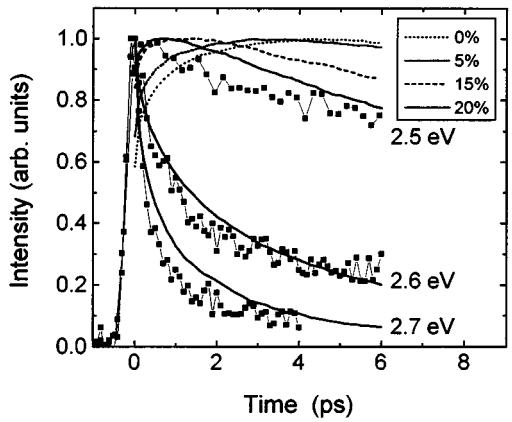

FIG. 4. Symbols show the transient luminescence of PPV at different emission energies at room temperature. The solid lines show the calculation of the transient luminescence for different emission energies and a trap density of 20%. The other lines show the expected luminescence transients at 2.5 eV for lower trap densities.

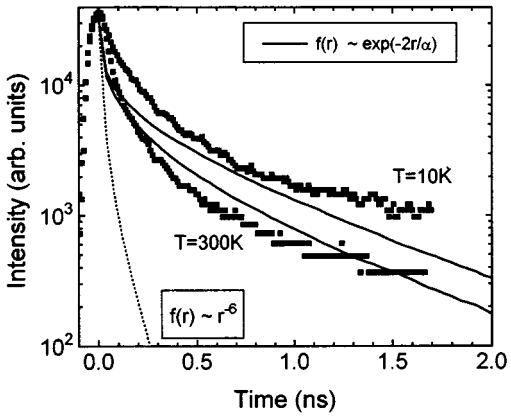

FIG. 5. Symbols show the luminescence decays of PPV recorded at different temperatures. The emission is detected at its spectral maximum. Lines show the calculated luminescence decay curves for different assumptions for the trapping process. A dipole-dipole transfer is assumed for the calculation of the dotted line, whereas the solid lines are based on the assumption of a phonon-assisted tunneling process.

We now turn over to the discussion of the excitation dynamics on a time scale of several hundred picoseconds to nanoseconds. We again compare the computed results with recent time-resolved fluorescence measurements on PPV performed by means of the streak-camera technique.[10] Figure 5 shows a comparison of the experimental nanosecond luminescence transient (measured at the luminescence maximum) with the simulated results. Again we consider an exponential as well as a $1/r^6$ distance dependence for hopping into the trap states. In both cases we use the parameters for the hopping process and the trap density as obtained from fitting the femtosecond luminescence data. As clearly seen in Fig. 5, the simulated luminescence decay in the case of the dipole-dipole coupling is much faster than the decays observed in the experiment. Better agreement is achieved using the assumption of an exponential dependence. Even the temperature dependence is well reproduced by our simulations. At higher temperatures the excitons are more mobile due to possible activated hops and thus reach traps more efficiently.

B. Discussion

For a more thorough discussion of the involved hopping processes it is useful to plot the negative logarithm of the normalized intensity on a logarithmic time axis. In this plot deviations from a Kohlrausch-Williams-Watts (KWW) behavior[30,31]

$$I(t) = I_0 \exp(-t/t_0)^{\beta} \tag{6}$$

can be found. If the relaxation follows a KWW law one gets a straight line with a slope of β .

The experimental transient luminescence detected at 2.6 eV is shown on a KWW plot in Fig. 6. The slope of the curve is close to 1 at early times and then it decreases for larger times. The calculated emission curves for this energy are shown in Fig. 6 for different scenarios. For all calcula-

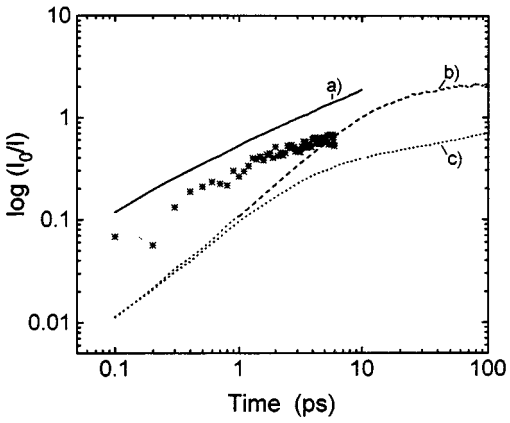

FIG. 6. KWW plot of the experimental luminescence transient at 2.6 eV (symbols) and calculated curves for different scenarios (lines). The solid line *a* is a calculation with exponentially dependent hopping rates in a three-dimensional model. A spatial disorder of 0.4 was assumed. For the calculation of the dashed and the dotted line dipole-dipole transfer was assumed. The dashed line *b* represents a calculation where a three-dimensional sample was simulated, whereas a one-dimensional sample was assumed for the calculation of the dotted line *c*. The parameter in both cases were chosen to fit the initial decay of the experimental luminescence data. For clarity, the different curves are arbitrarily shifted.

tions the parameters determining the hopping dynamics were chosen such that the high-energy luminescence decay at 2.7 eV was fitted. With the assumption of an exponential dependence for the hopping transfer and a three-dimensional model we obtain good agreement with the experimental data. For curve *a* in Fig. 6 a reasonable spatial disorder parameter of 0.4 was assumed. The slope and the characteristic turnover in the experimental data are nicely reproduced. The necessity for introducing spatial disorder in our simulations indicates that a broad distribution of hopping distances is involved even in the early stage of the relaxation process. This can be explained by the superposition of intra- and interchain processes as well as by the fact that PPV exhibits a rather complicated morphology with different degrees of crystallinity in different regions of the sample. Our optical experiment averages over all regions of the sample. The spatial disorder u is then an effective parameter that simulates the superpostion of the different microscopic hopping processes.

Despite the agreement found in the above comparisons, several additional aspects have to be considered during the interpretation of our results. We have not incorporated the local anisotropy of the polymer into our model. Albeit the macroscopic properties of the polymers are isotropic and no longe-range order exists, the polymer chain is locally one dimensional and thus the electronic wave functions are extended in only one direction. The relaxation processes partly take place on different conjugated segments of *one* polymer chain. It has been shown that these intrachain relaxation processes mainly occur on the time scale of less than 20 ps.[32] At larger times interchain processes dominate the relaxation dynamics. A refined model therefore has to take into account this interplay between intra- and interchain transfer processes.

The fact that the nature of the relaxation process is dominantly one dimensional during the first picoseconds is not only important for the calculation of the coupling between the different sites, but it also affects the relaxation dynamics itself.[14] For comparison we have carried out simulations for the case of dipole-dipole coupling assuming a three-dimensional as well as one-dimensional model. Curves *b* and *c* in Fig. 6 depict the results of these calculations. In agreement with previous results[7] achieved via different numerical techniques, we also find a characteristic turnover in the KWW plots. In the case of a one-dimensional model the calculated curve is very similar to the experimental data.

Another problem arises because at early times the excitations hop over small distances that are comparable to the exciton radius [$\sim 10-20$ Å (Ref. 33)]. The spatial separation of different chains is on the same order (<10 Å). In this case the condition for the application of the dipole approximation is not really fulfilled. Furthermore, we have to point out that our calculations were performed with the approximation of a constant value for the spectral overlap of the donating and the absorbing state independent on the energy of the states. Further work has to be done to clarify the hopping mechanisms on the time scale <20 ps.

A more definite conclusion can be drawn for the trapping process that controls the luminescence decay at longer times. Since this process is a three-dimensional process and additionally the average hopping distance on this time scale is larger, our model is well suited for the simulation of the trapping dynamics. The comparisons shown in Figs. 4 and 5 give strong evidence that the trapping process is mediated by a tunneling process. A probable candidate is tunneling of an electron to an extrinsic acceptor state, as suggested in recent luminescence and photoconductivity studies.[11,34] Our simulations are in good agreement with this scenario, where the luminescence quenching is due to the capture of the electron into an extrinsic trapping site with the hole remaining on the conjugated polymer chain. Due to the spatial separation of the two oppositely charged quasiparticles, the probability for radiative decay is low after trapping and hence competing nonradiative processes dominate. The quite high value of 20% for the trap density indicates efficient capture into the trap states. This is most likely due to the highly delocalized nature of the electronic wave function. Since the conjugation length in PPV is on the order of 10 repeat units, one defect on each 50th monomer unit results in an effective trap density of 20%.

In summary, the simulations presented in this section have shown that the experimental data can be understood in terms of an incoherent hopping motion of neutral photoexcitations between the different sites of the polymer. Albeit the details of the femtosecond relaxation dynamics are not yet fully understood, good agreement with a series of time-resolved luminescence measurements covering the femtosecond up to the nanosecond time scale is obtained by assuming an overall exponential dependence of the hopping rate on the distance between the sites. The importance of a trapping process has been pointed out. Assuming $\alpha = 6$ Å , the data are best fitted with the following values for the different parameters characterizing the hopping motion: $\nu_0 = 6.0 \times 10^{14}$ s^{-1}, $u = 0.4$, and 20% traps.

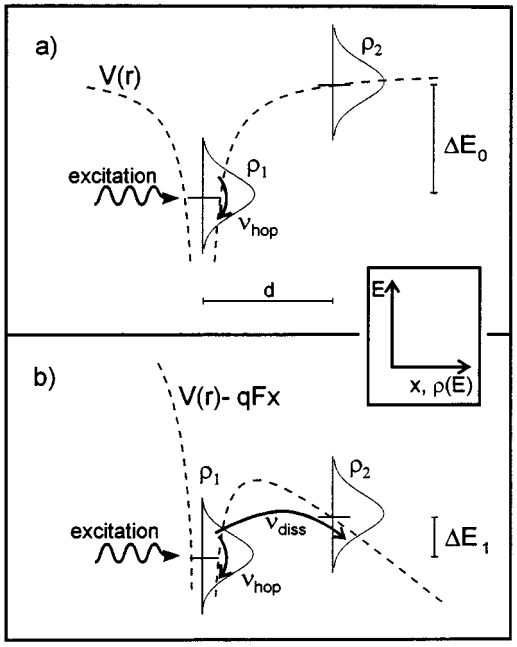

FIG. 7. Scheme of energy relaxation and the primary step of the dissociation of photoexcitations (a) without and (b) with applied electric field. ρ_1 is the DOS of the neutral excitations, while ρ_2 is the density of states of the geminate pairs, where one of the charges is spatially separated from its oppositely charged counterpart. ρ_2 is effectively lowered upon the application of an electric field.

IV. EXCITON DISSOCIATION

We now address the important issue of the transition from a neutral photoexcitation to a pair of charge carriers. The understanding of this process is of crucial importance for resolving the nature of the photoexcitations as well as for further improvement of organic photodetectors and solar cells. We extend our model in order to include the effect of an external electric field on the dynamics of the photoexcitations. We compare our calculations with recent experiments on the field-induced luminescence quenching measured in conjugated polymer diodes.[23,24,35,36] In these measurements a strong field effect on the photoluminescence was found. Upon applying an electric field of about 1.5×10^6V/cm the photoluminescence of the samples decreased to values as low as 20% of the value without electric field. This effect results from the field-induced dissociation of neutral photoexcitations in the electric field.

A scheme of the primary step in the dissociation process is sketched in Fig. 7: After photoexcitation with a short laser pulse with a photon energy significantly larger than the absorption threshold of the lowest optical $S_1\leftarrow S_0$ transition, ultrafast vibronic relaxation leads to a random occupation of the Gaussian DOS ρ_1 of the neutral S_1 states. We here assume that the vibronic relaxation is faster than any field-assisted hopping process. Each photoexcitation consists of a pair of oppositely charged quasiparticles on the same conjugated segment, bound by Coulomb interaction. We refer to this excitation as exciton in the following.

The subsequent dynamics of the photoexcited ensemble of excitons is determined by a superpostion of the following processes: (i) spectral relaxation in the DOS ρ_1 via hopping processes, (ii) trapping, (iii) radiative deactivation, and (iv) dissociation. Here dissociation is hopping of one carrier to a neighboring site, leading to the formation of a geminate pair (GP). The total energy of this GP is also a subject of inhomogeneous broadening. The adjacent DOS is depicted as ρ_2 in the scheme in Fig. 7. During the dissociation process the carrier has to overcome the difference ΔE_0 between the Coulombic binding energy E_B of the two charges located on the same conjugated segment and the remaining binding energy E_{GP} of the geminate pair with the charges spatially separated by a certain distance d. Without an applied electric field [Fig. 7 (a)] the dissociation process is quite improbable for a binding energy E_B higher than kT. Dissociation can only occur for excitons very high in DOS ρ_1 or via involvement of traps that capture one of the charges. A strong electric field changes the situation significantly, as depicted in Fig. 7(b). The Coulomb potential between the two charges is superimposed by the external electric field, affecting the total energy of a GP. The maximum change occurs for pairs whose dipole is oriented along the electric field. If we assume that one charge hops the distance d along the field direction, the energy gain due to the external electric field is $\Delta E_0-\Delta E_1=\Delta E_F=qFd$, where q is the charge and F the electric field. Thus DOS ρ_2 is effectively lowered and hence the dissociation process becomes more probable.

In our simulations each fully conjugated segment is represented by one pointlike site. The binding energy E_B of two charges at the same site (exciton) is kept as a fit parameter in our calculations. For each binding energy we calculate the exciton radius r_B determined by

$$\frac{e^2}{4\pi\epsilon_0\epsilon_r}\frac{1}{r_B}=E_B\,. \tag{7}$$

We here use $\epsilon_r=3.5$. The electrostatic potential of the geminate pair with two charges on different sites i and j is then a shifted $1/r$ potential, which is calculated according to

$$E_{\mathrm{GP}}(r_{ij})=\frac{e^2}{4\pi\epsilon_0\epsilon_r}\frac{1}{(r_B+r_{ij})}. \tag{8}$$

A more elaborate treatment is a model where the conjugated segments are assumed to be rodlike and consequently the charges are spread out over the whole segment. Deviations between the resulting potential and E_{GP} as defined in Eq. (8), however, are small compared to the width of the DOS. Additionally, our simulations have shown that the results are not very sensitive on the exact choice of the potential. For simplicity, we therefore use Eq. (8) for the calculation of the Coulomb attraction of a GP.

After the formation of a GP the subsequent evolution into a pair of free charge carriers is a process often described in terms of the Onsager model.[37] This is not included in our simulations. Only the primary but crucial step for the quenching of the luminescence is considered. In contrast to the hopping processes of the neutral excitation, no activated formation of a geminate pair is allowed in this case since the probability for the reformation of the exciton is high. On the other hand, an energetically favored formation of a GP by hopping of one charge to another site is always considered as a successful dissociation process since the probability for a further separation of the two charges is high compared to the

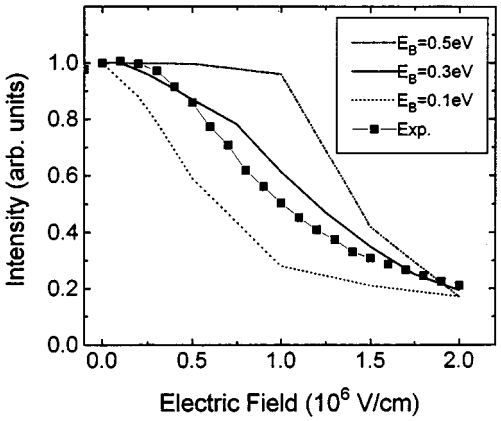

FIG. 8. Lines show the calculated values of the time-integrated luminescence as a function of the applied field for different assumptions for the exciton binding energy E_B. For comparison the experimentally determined values are also shown (symbols).

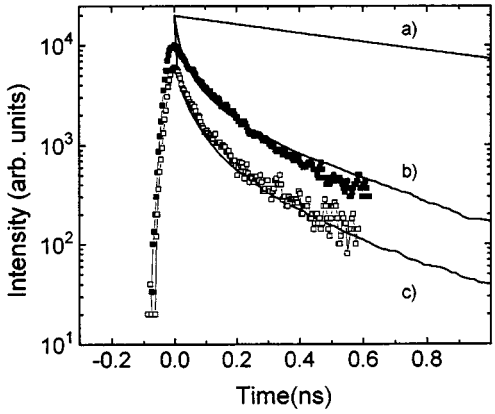

FIG. 9. Calculated transient integrated excitation densities for different scenarios: *a* only radiative recombination, *b* radiative recombination and trapping (the optimum parameter set as found in Sec. III was used), and *c* additional field-assisted dissociation of photoexcitations in an external electric field of 1.5×10^6 V/cm was considered. The symbols represent the experimental curves without (filled squares) and with (hollow squares) electrical field.

probability for the reformation of the exciton. In agreement with all these considerations, we extend the rate equations [Eq. (4)] for the inclusion of the dissociation process. For each site we consider the dissociation with a hop of one charge to a neighboring site to be a possible process. For an applied field in the x direction the additional rate $\nu_{\mathrm{diss},i}$ for the dissociation of an exciton at site i is given by

$$\nu_{\mathrm{diss},i}=\nu_{0,\mathrm{diss}}\sum_j \exp(-2r_{ij}/\alpha)\begin{cases}0, & \Delta E_{ij}<0\\ 1, & \Delta E_{ij}>0,\end{cases} \tag{9}$$

$$\Delta E_{ij}=E_i-E_B+E_{\mathrm{GP}}(r_{ij})+eFx_{ij}-E_j,$$
$$r_{ij}=|r_i-r_j|,$$
$$x_{ij}=x_j-x_i.$$

In this ansatz we assume implicitly that the distribution of energies is the same for excitons and charged carriers. This assumption is exactly fulfilled when the inhomogeneous broadening of the excitonic states is totally due to the energetic disorder of either the highest occupied molecular orbital (HOMO) or the lowest unoccupied molecular orbital (LUMO) states. In the more likely case that both levels are subject of inhomogeneous broadening, our simulations slightly underestimate the dissociation process.

Based on the results of Sec. III, an exponential distance dependence is assumed for the exciton transfer (spectral relaxation) to other sites, the trapping process, and also for the dissociation process. The only additional parameter then is $\nu_0/\nu_{0,\mathrm{diss}}$, the ratio of the prefactor for hopping of a neutral excitation (spectral relaxation) and a single charge (dissociation), respectively. In our calculations we used a ratio of 1, which is an upper limit since hopping of an exciton includes tunneling of two instead of one carrier as in the case of dissociation. For the comparison with the recently published data for the luminescence quenching in a PPV diode,[24] we have calculated the time-integrated as well as the time-resolved PL quenching for different parameters. In our simulations we assume a uniform electric field. A more refined analysis of the experiment has to consider the inhomogeneous electric field distribution near the polymer-metal interface. However, we do not expect any significant differences.

Figure 8 summarizes the results. We have calculated the field dependence of the PL versus the electric field for different values for the exciton binding energy E_B. Using the parameters found in Sec. III, we obtain the best agreement between simulated and experimental data for $E_B\sim0.3$ eV.

Independent support for the validity of our simulation stems from the comparison with time-resolved luminescence measurements. Figure 9 depicts the temporal evolution of the calculated spectrally integrated exciton densities for different scenarios (lines). The simulated data are compared with the time-resolved luminescence of a PPV diode without (filled squares, curve *b*) and with (hollow squares, curve *c*) applied electric field. For the calculation of curve *a* a trap-free sample was assumed. The luminescence decay in this case is solely determined by the radiative decay of the excitons. Depending on the exciton binding energy, there are also spontaneous dissociation processes of those excitons which are located high in the DOS. For $E_B>0.2$ eV, however, this process is only a minor effect. Curve *b* again shows the drastic effect of the traps on the exciton dynamics. Within the time resolution of the streak-camera measurement already a significant portion of the excitons decay nonradiatively. As discussed in Sec. III, this trapping process, which is probably a capture process of the electron, has to be considered for a proper description of the excitation dynamics. The capture of only one charge by a trapping site is more naturally included in the simulations when dissociation processes are allowed. In this framework the trapping process is just a spontaneous dissociation process where an electronic level deep in the gap is involved. Curve *c* in Fig. 9 is the result of the simulation of the luminescence dynamics considering traps and an electric field of 1.5×10^6 V/cm. The same parameters as in Fig. 8; i.e., an exciton binding energy of 0.3 eV, are assumed. The computed curve for the lumi-

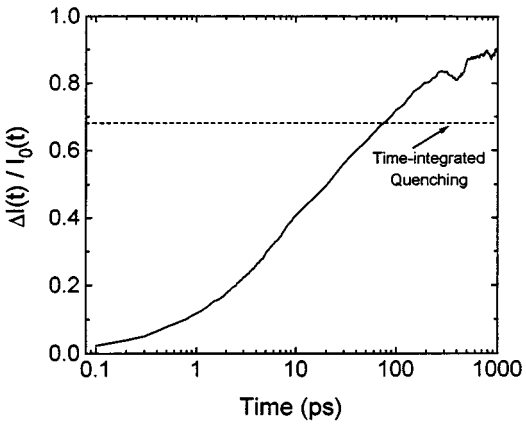

FIG. 10. Calculation of the time-resolved luminescence quenching for an electric field of 1.5×10^6 V/cm. The dashed line shows the integrated value of the PL quenching.

nescence decay with applied electric field agrees very well with the experimentally found behavior.

The above good agreement of the field dependence of the time-integrated PL quenching and the good fit of the time-resolved data with and without electric field strongly supports the parameter set used to describe the excitation dynamics in PPV. Our combined experimental and computational approach allows us to determine the value for E_B to 0.3 ± 0.1 eV. This is in agreement with recent theoretical predictions stressing the role of the Coulomb interaction in conjugated polymers.[38,22,39] There is particularly good agreement with the value found in local-density functional band structure calculations[38] for PPV, which result in an exciton binding energy of 0.4 ± 0.1 eV.

The quenching due to the dissociation is a time-dependent process. This can be understood as follows. As long as the higher-lying states in the DOS ρ_1 of the neutral excitations are occupied, the probability for dissociation is quite high. This gives a certain initial average dissociation rate, which leads to a dynamic decrease of the exciton density. In parallel to the spectral relaxation of the excitons, the overall rate for dissociation events decreases.

It is particularly interesting to study the field-dependent time evolution with femtosecond time resolution since most of the dissociation events occur in an early stage after photoexcitation. In Fig. 10 we plot the calculated time-resolved PL quenching $[I_0(t)-I_F(t)]/I_0(t)$. On this time scale the dissociation dynamics can be fully resolved. Only a few dissociation events occur within the first picosecond. After 1 ps the curve gets steeper and quenching values of the same order as measured in the time-integrated measurements are reached within the first 50 ps. On this logarithmic time scale the curve flattens again for longer times, reflecting the fact that the spectral relaxation has led to a predominant occupation of excitonic states that are low in energy. We point out that a very similar behavior was found experimentally in a phenyl-substituted derivative of PPV blended into polycarbonate.[23] Since basically the same physics is expected to occur in that system, we have further evidence that our simulations describe the dissociation dynamics very well.

V. CONCLUSION

We have presented a comprehensive comparison of Monte Carlo simulations and experimental results on the relaxation and dissociation of photoexcitations in the conjugated polymer PPV. We found that the emission behavior on all time scales can be fitted by assuming that the hopping rates determining the spectral relaxation depend exponentially on the distance between the two sites involved. The evolution of the luminescence on a longer time scale is determined by a trapping process. Our simulations indicate that about 20% of all sites act as trapping sites. This trapping most likely occurs by tunneling of one of the charges forming the neutral photoexcitation.

Our study of the field-induced dissociation of the excitons reveals all the characteristics found in the experiments. Based on the same parameters used for the simulation in the field-free case, we used the exciton binding energy E_B of two charges located at the same point as a fitting parameter. Our calculations show that the binding energy is $E_B\approx 0.3$ eV.

ACKNOWLEDGMENTS

We gratefully acknowledge the funding by the Deutsche Forschungsgemeinschaft through the Sonderforschungsbereich 383. Our computational work was supported by a grant for CPU time at the Supercomputing Facilities at the Forschungszentrum KFA Jülich. We thank S. Baranovskii, S. W. Koch, M. Deussen, and A. J. Heeger for fruitful discussions and K. Bott for technical assistance.

*Present address: LH-Systems, Frankfurt, Germany.
†Present address: Sektion Physik, Ludwig-Maximilians Universität München, Amalienstrasse 54, 80799 München, Germany. Author to whom correspondence should be addressed.
‡Present address: Institut für Physikalische Chemie der Universität Wien, Austria.
§Present address: IBM Almaden Research Center, San Jose, CA.
‖Present address: IBM Research Division, Rüschlikon, Switzerland.
¶Present address: Physikalisch-Technische Bundesanstalt, Braunschweig, Germany.

[1] *Relaxation in Polymers*, edited by T. Kobayashi (World Scientific, Singapore, 1993).
[2] R. Friend, D. D. C. Bradley, and A. Holmes, Phys. World **5** (11), 42 (1992).
[3] J. H. Burroughes *et al.*, Nature **347**, 539 (1990).
[4] J. M. Leng *et al.*, Phys. Rev. Lett. **72**, 156 (1994).
[5] M. Yan *et al.*, Phys. Rev. Lett. **73**, 744 (1994).
[6] K. Pakbaz *et al.*, Synth. Met. **64**, 295 (1994).
[7] B. Mollay *et al.*, Phys. Rev. **B 50**, 10 769 (1994).
[8] U. Rauscher, H. Bässler, D. D. C. Bradley, and M. Hennecke, Phys. Rev. B **42**, 9830 (1990).
[9] R. Kersting *et al.*, Phys. Rev. Lett. **70**, 3820 (1993).
[10] U. Lemmer *et al.*, Appl. Phys. Lett. **62**, 2827 (1993).
[11] M. Yan *et al.*, Phys. Rev. Lett. **72**, 1104 (1994).

[12] B. Movaghar *et al.*, Phys. Rev. B **33**, 5545 (1986).
[13] B. Mollay and H. F. Kauffmann, J. Chem. Phys. **97**, 4380 (1992).
[14] A. Blumen, J. Chem. Phys. **72**, 2632 (1980).
[15] A. Blumen, G. Zumofen, and J. Klafter, Phys. Rev. B **30**, 5379 (1984).
[16] R. Brown and C. von Borczyskowski, Chem. Phys. **170**, 57 (1993).
[17] *Conjugated Conducting Polymers*, edited by H. G. Kiess (Springer, Berlin, 1992).
[18] A. J. Heeger, S. Kivelson, J. R. Schrieffer, and W. P. Su, Rev. Mod. Phys. **60**, 781 (1988).
[19] K. Lochner, H. Bässler, B. Tieke, and G. Wegner, Phys. Status Solidi B **88**, 653 (1978).
[20] G. Weiser, Phys. Rev. B **45**, 14 076 (1992).
[21] C. H. Lee, G. Yu, D. Moses, and A. J. Heeger, Phys. Rev. B **49**, 2396 (1994).
[22] M. Chandross *et al.*, Phys. Rev. B **50**, 14 702 (1994).
[23] R. Kersting *et al.*, Phys. Rev. Lett. **73**, 1440 (1994).
[24] U. Lemmer *et al.*, Synth. Met. **67**, 169 (1994).
[25] R. F. Mahrt *et al.*, Macromol. Chem. **11**, 415 (1990).
[26] A. Miller and E. Abrahams, Phys. Rev. **120**, 745 (1992).
[27] T. Foerster, Ann. Phys. (Leipzig) **6**, 55 (1948).
[28] G. Schönherr, H. Bässler, and M. Silver, Philos. Mag. B **44**, 47 (1981).
[29] F. Rossi, P. Poli, and C. Jacoboni, Semicond. Sci. Technol. **7**, 1017 (1992).
[30] G. Williams, Adv. Polym. Sci. **33**, 59 (1979).
[31] J. Klafter and A. Blumen, Chem. Phys. Lett. **119**, 377 (1985).
[32] U. Lemmer *et al.*, Chem. Phys. Lett. **209**, 243 (1993).
[33] A. Horvath, H. Bässler, and G. Weiser, Phys. Status Solidi B **173**, 755 (1992).
[34] H. Antoniadis *et al.*, Phys. Rev. **50**, 14 911 (1994).
[35] M. Deussen, M. Scheidler, and H. Bässler, Synth. Met. **73**, 123 (1995).
[36] V.I. Arkhipov *et al.*, Phys. Rev. B **52**, 4932 (1995).
[37] L. Onsager, Phys. Rev. **54**, 554 (1938).
[38] P. Gomes da Costa, and E.M. Conwell, Phys. Rev. B **48**, 1993 (1993).
[39] M. Hartmann, V. Chernyak, and S. Mukamel, Phys. Rev. B **52**, 2528 (1995).